Characteristics of a UF_6-H_2/HF nuclear-pumped laser

M. J. Kushner [a)]
California Institute of Technology, Pasadena, California 91125

(Received 22 Obtober 1979; accepted for publication 7 January 1980)

Nuclear pumped lasers are characterized by high-threshold neutron fluxes and low gain. This is due primarily to the fact that the fissile gas, which has the largest partial pressure and hence has the largest fraction of fission energy deposited in it, is not the lasing species. The closer the fissile gas can be coupled to the actual lasing process, the more efficient the laser will be. In this paper, a model for a potential new nuclear-pumped HF laser is presented. Using a $^{235}UF_6$-H_2 gas mixture, a peak gain of about 50%/m and a threshold neutron flux of $< 10^{14}/cm^2$ s are predicted. Recommendations are made concerning optimum use of the new system.

PACS numbers: 42.60.By, 42.55.Ks, 28.90. + i

I. INTRODUCTION

One of the major problems of scaling conventional electric discharge, e-beam, or chemical lasers to large dimensions is uniformly depositing energy throughout the active volume. Nuclear-pumped lasers (NPL) provide a potential solution to this problem. A nuclear-pumped laser converts the kinetic energy of fission fragments (FF) produced by fission reactions into electromagnetic energy. Since the mean free path of thermal neutrons through fissile gas mixtures can be many meters long, a large volume of gas can be uniformly pumped.

There have been two successful techniques for achieving laser action with nuclear pumping. With the first method, fissile material is contained in a coating or foil which lines the inside of the laser tube. With a boron-impregnated foil, the $^1n(^{10}B, \alpha)^7$ Li reaction has produced laser action in mercury,[1] nitrogen,[2] and carbon.[3] With foils containing uranium, the more energetic $^1n(^{235}U, FF)FF$ reaction has produced laser action in carbon monoxide[4] and xenon.[5] Because the source of fission fragments is external to the gas mixture, as the tube radius or gas pressure become large, the fission energy is no longer deposited uniformly.[6] The second technique uses a fissile gas as the source of fission fragments and therefore is not subject to the same limitatons. The $^3He(n, p)^3H$ reaction has produced laser action or optical gain in oxygen,[7] argon,[8] krypton,[9] and xenon.[9] The source of neutrons for either method is a pulsed nuclear reactor having a peak flux of 10^{14}–10^{17} neutrons/cm^2 s.

In present nuclear-pumped lasers, the source of fission fragments is not the lasing gas. The most direct participaton in the lasing process that the fissile gas has had is in systems similar to the ^{3}He-Ar NPL. In this system, argon is pumped by charge-exchange collisions with molecular helium ions.[10] The fissile gas in a volumetrically pumped laser usually has the largest partial pressure, and therefore most of the fission energy is deposited in that gas. Therefore, if the number of steps required to transfer the fission energy from the fissile gas to the lasing gas can be reduced, the laser will be more efficient.

In this paper, a new nuclear-pumped system is investigated in which the coupling between the fissile gas, $^{235}UF_6$, and the lasing species, HF, is more direct. The proposed system uses a $^{235}UF_6$-H_2 gas mixture. Fission fragments from $^1n(^{235}U, FF)FF$ reactions dissociate the UF_6, producing fluorine atoms. The fluorine atoms then react with hydrogen to form HF. Therefore, the UF_6 is only one step removed from the pumping reaction. The results of a computer model show that the optical gain in this system is as large or larger than for any present NPL, while the threshold neutron flux is lower than any present NPL. The gain produced in this system is for transitions between the first few vibrational levels of the ground electronic state of HF and is rapidly quenched by H_2-HF, UF_6-HF, and HF-HF vibrational-translational (VT) collisions, and HF-HF vibrational-vibrational collisions (VV). The gain is therefore a sensitive function of both temperature, pressure, and the rate of rise of the neutron flux. The sensitivity of gain to these quantities will be discussed.

II. THE MODEL

Uranium hexafluoride (UF_6) and molecular hydrogen (H_2) flow through a laser tube. The tube is either part of a nuclear reactor or placed in the vicinity of a nuclear reactor capable of producing neutron fluxes of 10^{12}-10^{17} neutrons/cm^2 s. When the reactor is pulsed, high-energy neutrons are produced and subsequently moderated to thermal energies. The fission reaction

$$n + {}^{235}UF_6 \rightarrow 2FF \tag{1}$$

liberates 207 MeV of energy. Most of this energy appears as kinetic energy in a light fission fragment (98 MeV) and a heavy (67 MeV) fission fragment. While slowing down, the fission fragments deposit their energy in the gas, causing ionizations, excitations, and dissociations. Fluorine atoms which are dissociated from the UF_6 react with the hydrogen, creating nonequilibrium hydrogen fluoride;

$$F + H_2 \rightarrow H + HF(v), \quad v = 1, 2, 3. \tag{2}$$

The first three vibrational levels of HF are populated in the ratio 1:3.4:1.7,[11] creating an inversion and hence optical gain.

The following species are considered:

uranium hexafluoride $\quad {}^{235}UF_6$, $^{238}UF_6$

[a)]Present address: Sandia Laboratories, Albuquerque, New Mexico 87185.

 0021-8979/80/052421-08$01.10

hydrogen H_2, H
fluorine F_2, F
hydrogen fluoride HF(v)
neutrons n
gas temperature T_g.

The manner in which fission energy is deposited in the gas is described using the treatment by Wilson and DeYoung.[12] The energy deposited at a distance r from the centerline of a tube of radius b by fission fragment i in gas component j is

$$\mathscr{E}_j^i(r) = \nu_j^i \frac{E_F^i}{l}\varphi\frac{1}{6}\sum_{k=1}^{6}\left\{1+\frac{R_0^i(\theta_k)}{R_F^i}\cos^{-1}\left(\frac{R_0^i(\theta_k)}{R_F^i}\right) - \left[1-\left(\frac{R_0^i(\theta_k)}{R_F^i}\right)^2\right]^{1/2}\right\}, \quad (3)$$

where $\theta_k = \frac{1}{3}(k-1)\pi$, E_F^i is the initial energy of the fission fragment, l is the neutron mean free path, and φ is the thermal neutron flux. The neutron mean free path is given by $l = 0.237(T_g/P_{UF_6})$ cm, where P_{UF_6} is the $^{235}UF_6$ pressure in atmospheres and the gas temperature is in °K.[13] The range of fission fragment i in the gas mixture, R_F^i, is given by

$$\frac{1}{R_F^i} = \sum_j \frac{n_j}{R_{F_j}^i}, \quad (4)$$

where $R_{F_j}^i$ is the range of fission fragment i per molecule/cm^3 of gas j and n_j is the gas density. In Eq. (3)

$$R_0(\theta) = (b^2 - r^2\sin^2\theta)^{1/2} - r\cos\theta. \quad (5)$$

If $R_0(\theta)$ exceeds R_F^i, then $R_0(\theta) = R_F^i$. The fraction of the energy of fission fragment, i, E_F^i, deposited in gas j is ν_j^i where

$$\nu_j^i = \frac{P_j}{R_{F_j}^i\sum_k P_k/R_{F_k}^i}, \quad (6)$$

where P_j is the partial pressure of gas j. Of the fission fragment energy deposited in gas j, a fraction β_j results in dissociations. Therefore, the rate of production of F atoms due to nuclear pumping is

$$\frac{\partial[\mathrm{F}]}{\partial t} = \sum_i \frac{\mathscr{E}^i_{UF_6}\beta_{UF_6}}{\gamma_F}, \quad (7)$$

where γ_F is the average bond energy of an F atom in UF_6 ($\gamma_F \simeq 124$ kcal/mode [14]).

The time rate of change of $HF(v=i)$ is given by

$$\begin{aligned}\frac{dN_i}{dt} &= (M_F M_{H_2} r_1^i - N_i M_H r_{-1}^i) + (M_H M_{F_2} r_2^i - N_i M_F r_{-2}^i)\\
&- \sum_j\left[N_iN_j - N_{i-1}N_{j+1}\exp\left(-\frac{(E_{j+1}-E_j)-(E_i-E_{i-1})}{kT_g}\right)\right]r_{VV}^{i,j}\\
&+ \sum_j\left[N_{j+1}N_j - N_iN_{j+1}\exp\left(-\frac{(E_{j+1}-E_j)-(E_{i+1}-E_i)}{kT_g}\right)\right]r_{VV}^{i+1,j}\\
&- \sum_{k,j}\left[N_iM_k^j - N_{i-1}M_k^{j+1}\exp\left(-\frac{(E_{j+1}-E_j)-(E_i-E_{i-1})}{kT_g}\right)\right]r_{k,VV}^{i,j}\\
&+ \sum_{k,j}\left[N_{i+1}M_k^j - N_iM_k^{j+1}\exp\left(-\frac{(E_{j+1}-E_j)-(E_{i+1}-E_i)}{kT_g}\right)\right]r_{k,VV}^{i+1,j}\\
&- \left[N_i - N_{i-1}\exp\left(-\frac{E_i-E_{i-1}}{kT_g}\right)\right]\sum_k M_k r_{k,VT}^i - \left[N_{i+1} - N_i\exp\left(-\frac{E_{i+1}-E_i}{kT_g}\right)\right]\sum_k M_k r_{k,VT}^{i+1}\\
&- N_iA_{1,i} - N_iA_{2,i} + N_{i+1}A_{1,i+1} + N_{i+2}A_{2,i+2} - \frac{D_{HF}N_i}{\Lambda^2} - \frac{N_i}{T_g}\frac{dT_g}{dt},\end{aligned} \quad (8)$$

where N_i is the density of HF in vibrational level i, E_i is the energy of vibrational level i, M_k is the density of species k, and M_k^i is the density of species k in vibrational level i. The first term on the right-hand side of Eq. (8) describes the pumping reaction (2) having rate constant r_1, and its reverse reaction with rate constant r_{-1}. The second term describes the production of N_i by the reaction

$$F_2 + H \rightarrow HF(v) + F, \quad v = 0, 1, 2, \ldots, 8. \quad (9)$$

Reaction (9) makes a small contribution to the HF density because of the small density of F_2. This situation may be artifical. It was assumed that only F atoms are produced as products in a UF_6 dissociation. This assumption is consistent with the observation that laser emission occurs only for $v \leqslant 3$ in HF lasers using a UF_6-H_2 gas mixture and flashlamps to dissociate the UF_6.[15,16] This suggests that very few F_2 molecules are produced in the dissociations. If a significant amount of F_2 results from FF bombardment of UF_6, then reaction (9) will be important.

The third and fourth terms of Eq. (8) describe the time rate of change in N_i due to VV collisions with other HF molecules. The rate constant $r_{VV}^{i,j}$ is for collisions where

$$N_i + N_j \rightarrow N_{i-1} + N_{j+1}. \quad (10)$$

It will be shown that this term plays a major role in quenching gain and dictates the requirement that the neutron pulse rise rapidly for maximum gain.

The fifth and sixth terms of Eq. (8) describe VV reactions of N_i whith species M_k^i with rate constant $r_{k,VV}^{i,j}$. The only species besides HF considered for vibrational exchange is H_2. The vibrational levels of H_2 were taken to be in thermal equilibrium with the gas temperature.

Vibrational-translational reactions where

$$N_i + M_k \rightarrow N_{i-1} + M_k \quad (11)$$

with rate constant $r_{k,VT}^i$ are described by the seventh and eighth terms of Eq. (8). Because high pressures are required for fission energy to be deposited efficiently, VT reactions are a major quenching mechanism. The next four terms of Eq. (8) describe the change in N_i due to fundamental and first overtone spontaneous emission, with rates $A_{1,i}$ and $A_{2,i}$. The next term of Eq. (8) describes the loss of N_i due to diffusion with rate constant D and diffusion length Λ. This term makes a small contribution due to the high operating pressure. The last term, the change in density due to gas heating, does not appear if the number density instead of the pressure is kept constant.

The time rates of change in the densities of H_2 and H are given by

$$\begin{aligned}\frac{dM_{\mathrm{H}_2}}{dt} = & -\sum_i \frac{\mathscr{E}^i_{\mathrm{H}_2}\beta_{\mathrm{H}_2}}{\gamma_{\mathrm{H}}} - \sum_i (M_{\mathrm{F}} M_{\mathrm{H}_2} r^i_1 - M_{\mathrm{H}} N_i r^i_{-1}) \\ & - (M_{\mathrm{H}_2} M_{\mathrm{H}_2} r_3 - M_{\mathrm{H}} M_{\mathrm{H}} M_{\mathrm{H}_2} r_{-3}) \\ & - (M_{\mathrm{H}_2} M r_4 - M_{\mathrm{H}} M_{\mathrm{H}} M r_{-4}) \\ & - (M_{\mathrm{H}_2} M_{\mathrm{H}} r_5 - M_{\mathrm{H}} M_{\mathrm{H}} M_{\mathrm{H}} r_{-5}) \\ & + \frac{D_{\mathrm{H}} M_{\mathrm{H}}}{2\Lambda^2} - \frac{M_{\mathrm{H}_2}}{T_g}\frac{dT_g}{dt}, \end{aligned} \quad (12)$$

$$\begin{aligned}\frac{dM_{\mathrm{H}}}{dt} = & \sum_i \frac{2\mathscr{E}^i_{\mathrm{H}_2}\beta_{\mathrm{H}_2}}{\gamma_{\mathrm{H}}} \\ & - \sum_i (M_{\mathrm{H}} M_{\mathrm{F}_2} r^i_2 - N_i M_{\mathrm{F}} r^i_{-2} + N_i M_{\mathrm{H}} r_{-1}) \\ & + (M_{\mathrm{H}_2} M_{\mathrm{H}_2} r_3 - M_{\mathrm{H}} M_{\mathrm{H}} M_{\mathrm{H}_2} r_{-3}) \\ & + (M_{\mathrm{H}_2} M r_4 - M_{\mathrm{H}} M_{\mathrm{H}} M r_{-4}) \\ & + (M_{\mathrm{H}_2} M_{\mathrm{H}} r_5 - M_{\mathrm{H}} M_{\mathrm{H}} M_{\mathrm{H}} r_{-5}) \\ & - \frac{D_{\mathrm{H}} M_{\mathrm{H}}}{\Lambda^2} - \frac{M_{\mathrm{H}_2}}{T_g}\frac{dT_g}{dt}, \end{aligned} \quad (13)$$

The first terms of Eqs. (12) and (13) describe the energy deposited by fission fragments and are analogous to reaction (7) for fluorine. The second terms describe the pumping reactions for N_i. The next three terms are for the dissociation and reassociation reactions

$$H_2 + H_2 \rightleftarrows 2H + H_2, \quad (14a)$$

$$H_2 + M \rightleftarrows 2H + M, \quad (14b)$$

$$H_2 + H \rightleftarrows 3H, \quad (14c)$$

where M is any third body except H_2 or H. These reactions, as well as the last terms describing diffusion and thermal expansion, make small contribuions compared to the first two terms and are included for completeness only. The expressions for F_2 and F are analogous to Eqs. (12) and (13) where reaction (7) is included in the expression for F. Since $N_{\mathrm{F}_2} \ll N_{\mathrm{H}_2}$, and $N_{\mathrm{F}_2} \ll N_{\mathrm{UF}_6}$, any fission energy deposited in F_2 was ignored.

Due to the high pressure of UF_6, the densities of $^{235}UF_6$ and $^{238}UF_6$ remain nearly constant. Any dissociation products of UF_6 other than F were ignored. With this assumption, changes in the UF_6 densities are simply

$$\begin{aligned}\frac{dM_{^{235}\mathrm{UF}_6}}{dt} = & - M_{^{235}\mathrm{UF}_6}\varphi\sigma_f - \sum_i \frac{\mathscr{E}^i_{\mathrm{UF}_6}\alpha\beta_{\mathrm{UF}_6}}{\gamma_{\mathrm{F}}} \\ & - \frac{M_{^{235}\mathrm{UF}_6}}{T_g}\frac{dT_{\mathrm{gas}}}{dt}, \end{aligned} \quad (15)$$

$$\frac{dM_{^{238}\mathrm{UF}_6}}{dt} = -\sum_i \frac{\mathscr{E}^i_{\mathrm{UF}_6}(1-\alpha)\beta_{\mathrm{UF}_6}}{\gamma_{\mathrm{F}}} - \frac{M_{^{238}\mathrm{UF}_6}}{T_g}\frac{dT_g}{dt}, \quad (16)$$

where σ_f is the thermal fission cross section ($\sigma_f = 577 \times 10^{-24}\ \mathrm{cm}^2$ [13]) and α is the enrichment. Additional reactions such as[16,17]

$$H + UF_6 \rightarrow HF + UF_5, \quad \Delta H \approx -46\ \text{kcal/more}, \quad (17)$$

$$H_2 + UF_6 \rightarrow 2HF + UF_4 \quad (18)$$

were ignored.[18] The exothermicity of reaction (17) is sufficient to populate the fourth vibrational level of HF and therefore may also be a pumping reaction.[14]

It was assumed that fission energy which does not cause dissociations heats the gas mixture. This can be cosnidered a worst-case analysis as much of this energy causes ionizations and excitations. Nevertheless, the change in gas temperature turns out to be small during the period of positive gain. The time rate of change in gas temperature is

$$\begin{aligned}\frac{dT_g}{dt} = \frac{1}{(\Sigma_k M_k c_{p_k})}\bigg(& \frac{-hA_s(T_g - T_W)}{V} \\ & + \sum_{i,k} \mathscr{E}^i_k(1-\beta_i) + \sum_{i,k} N_i M_k r^i_{k,\mathrm{VT}}\Delta\epsilon^i\bigg), \end{aligned} \quad (19)$$

where h is the heat transfer coefficient, A_s is the surface area of the tube, V is the volume of the tube, and T_W is the wall temperature. The terms of Eq. (19) describe conduction of heat to the wall, energy deposited by fission fragments, and energy ($\Delta\epsilon^i$) transferred to the gas during VT collisions. The heat capacity of the gas component k is c_{p_k}.

The range of fission fragments in UF_6 and H_2 are listed in Table I. The rate constants for the pumping reactions and their inverses, as well as the VV rates, and VT rates for HF, H_2, F_2, and F were taken from the compilation by Cohen.[11] The VT rate for UF_6 was estimated to be the same as for SF_6.[19] Spontaneous emission coefficients for HF(v) were taken from the work of Herbelin and Emanuel.[20] The thermodynamic properties of UF_6 can be found in Refs. 21 and 22. The remaining heat capacities were taken from the JANAF tables.[23]

Gain for the vibrational rotational transition $N_{vj} \rightarrow N_{v-1,j'}$ can be calculated from the expression[24]

$$\gamma^{vj}_{v-1,j'} = \frac{\lambda^2}{8\pi} A^{vj}_{v-1,j'}\, g(\nu)\left(N_{vj} - N_{v-1,j'}\frac{g_{vj}}{g_{v-1,j'}}\right), \quad (20)$$

where $g(\nu)$ is the line-shape function and g_{vj} is the degeneracy of the level. At each time step, the maximum gain for a P-branch transition is calculated. The values of gain for a particular vibrational transition discussed in Sec. III therefore do not necessarily refer to the same rotational line.

TABLE I. Range of fission fragments in UF_6 and H_2. (The range is obtained by dividing the value in the table by the gas density.)

Fission fragment	Range in UF_6 (Ref. 12)	Range in H_2 (Ref. 26)
Light	$1.18 \times 10^{19}/\mathrm{cm}^2$	$1.23 \times 10^{20}/\mathrm{cm}^2$
Heavy	$1.05 \times 10^{19}/\mathrm{cm}^2$	$1.00 \times 10^{20}/\mathrm{cm}^2$

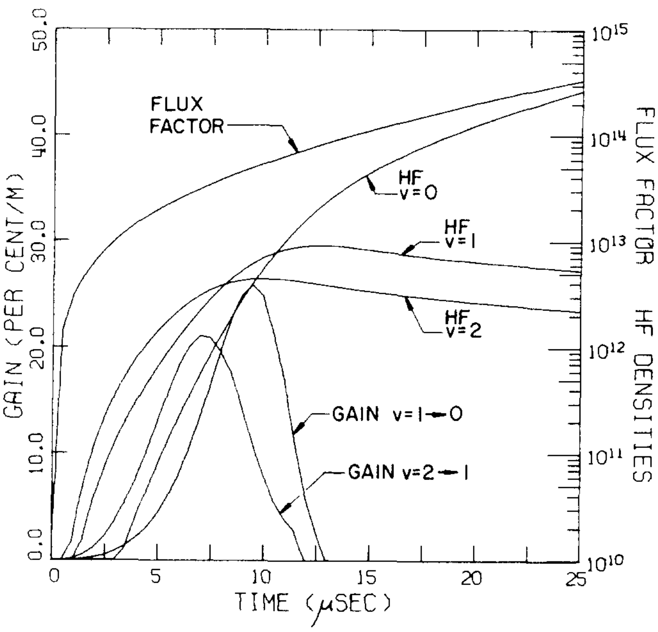

FIG. 1. Results for a neutron pulse in a UF_6-H_2 gas mixture. The densities are per cm^3. The flux factor has units of neutrons/cm^2 s, and has a peak value of 2×10^{15}. The total pressure is 0.4 atm and the fraction of hydrogen is 1.3%.

In previous models of nuclear-pumped lasers and plasmas, a constant neutron flux was assumed.[10,25] Nuclear-pumped lasers usually operate as long as the neutron flux is above threshold so that a quasi-steady-state assumption is justified. UF_6-H_2 system proposed here does not display this behavior and on the contrary is a sensitive function of the shape of the neutron pulse. Pulsed nuclear reactors which have been used for NPL have neutron pulses which are roughly Gaussian in shape with a FWHM from 60 μs to 15 ms.[1-4] Therefore, a Gaussian was assumed for the time dependence of the neutron flux. The FWHM and peak flux were kept as free paramenters.

For otherwise constant conditions, the rate of formation of HF is proportional to $\alpha\beta\varphi$ where α is the UF_6 enrichment, β is the fraction of the fission energy deposited which results in dissociations, and φ is the time-dependent neutron flux. For the range of conditions considered here, doubling the flux and halving the enrichment causes a negligible change in the results. Similarly, doubling the flux while halving β changes the results little. The actual value of β is at present unknown. Therefore, in the discussion which follows, the neutron flux is referred to as the "flux factor," $\Phi = \alpha\beta\varphi$. Φ has the same units as the actual flux φ, but gives a more realistic indication as to the pumping power of the neutron flux.

III. RESULTS AND DISCUSSION

Typical results showing gain and densities at the centerline of a tube for a neutron pulse in a UF_6-H_2 mixture are shown in Fig. 1. The total pressure is 0.4 atm, the initial gas temperature is 500 °K, and the fraction of hydrogen is 1.3%. The neutron pulse has a FWHM of 60 μs and the peak flux factor is 2×10^{15} neutrons/cm^2 s. (The pressure and fraction of hydrogen yield maximum gain for the particular choice of peak flux factor and pulse width.) Note that peak gain occurs for the $v = 1 \rightarrow 0$ transition ($j = 3$) and has a value of about

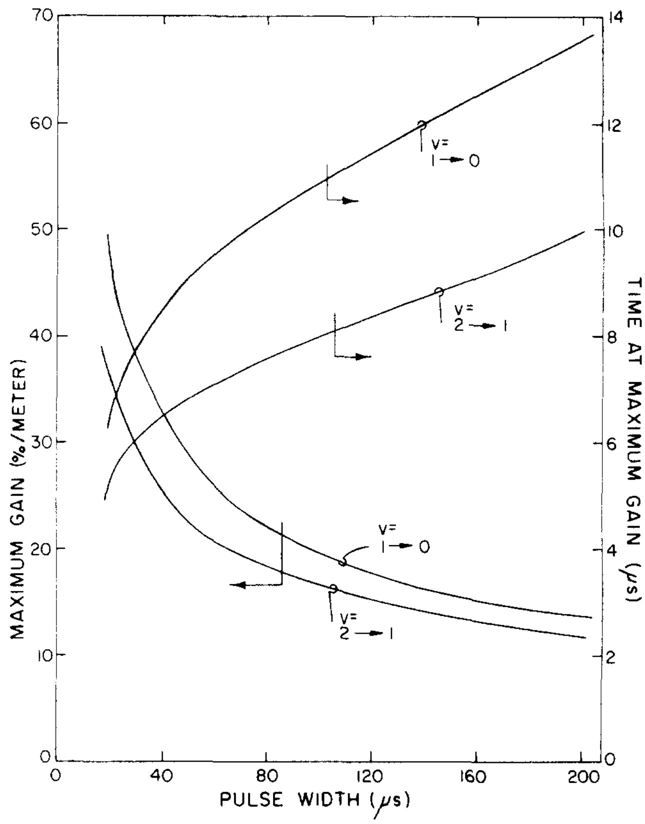

FIG. 2. Maximum gain and the time after the beginning of the neutron pulse that maximum gain occurs as a function of the width of the neutron pulse. The peak flux factor for each case is 2×10^{15} neutrons/cm^2 s. The total pressure is 0.4 atm and the fraction of hydrogen is 1.3%. The quenching time is only a function of pressure. Hence, a more rapidly rising neutron pulse populates the upper levels more heavily before the quenching time passes. The efficiency, though, decreases as the width decreases.

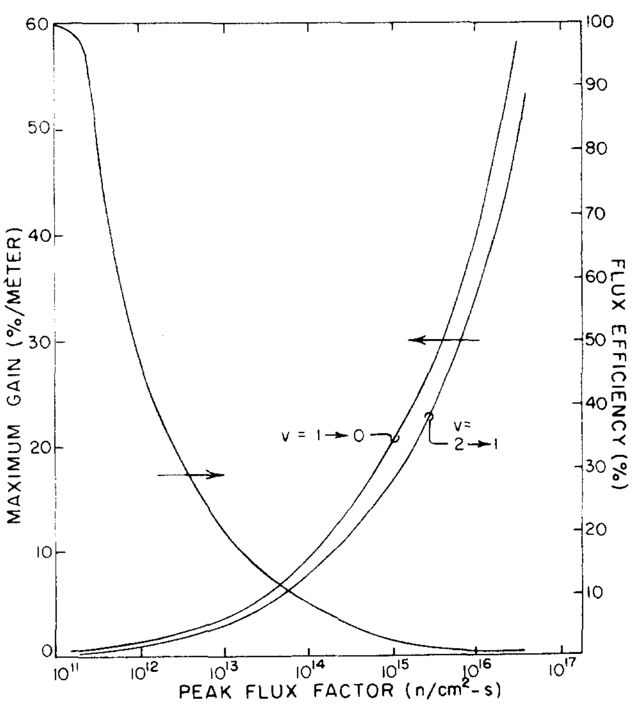

FIG. 3. Maximum gain and flux efficiency as a function of peak flux factor. The width of the neutron pulse is constant at 60 μs. Total pressure is 0.4 atm and the fraction of H_2 is 1.3%. As the peak flux factor increases, the maximum gain increases, but the flux efficiency and length of time of positive gain decreases.

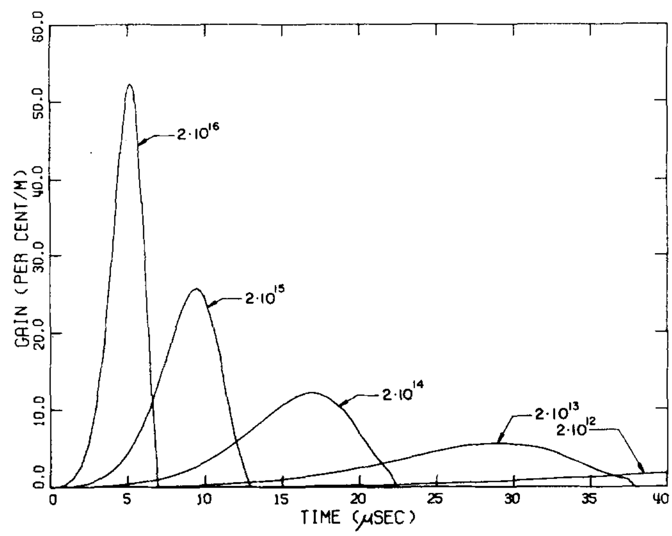

FIG. 4. Gain for the $v = 1 \rightarrow 0$ transition as a function of the time after the start of the neutron pulse and the peak flux factor for a pulse width of $60\,\mu s$. The conditions are the same as Fig. 3. As the peak flux factor decreases the HF-HF quenching rate decreases. Gain then is quenching primarily by UF_6 VT collisions. The length of time which gain is positive approaches the length of the neutron pulse.

26%/m. Maximum gain for the $v = 2 \rightarrow 1$ transition is about 21%/m ($j = 3$). Gain is never positive for the $= 3 \rightarrow 2$ transition. At the beginning of the neutron pulse, there is no HF. As the flux rises, gain is initially largest on the $2 \rightarrow 1$ transition because of the branching ratio which favors the second vibrational level. Initially, the dominant quenching mechanism is UF_6-HF VT collisions. Since this quenching rate is constant, as the flux increases, gain increases. But when the density of ground state HF exceeds a few times $10^{12}/cm^3$, the dominant quenching mechanism changes to VT and VV collisions with ground-state HF. As the flux increases, the rate of formation of excited HF increases, but the rate of formation of ground-state HF (and hence the quenching rate) increases even more rapidly. Eventually the quenching rate dominates and positive gain can no longer be sustained.

Note that during the neutron pulse, the maximum gain occurs at about $10\,\mu s$ when the flux factor is only 2% of its peak value. For a given pressure of UF_6, there is a quenching time, τ_q, which must pass before the density of ground-state HF becomes comparable to the upper levels. This time is on the order of the inverse of the quenching rate, $\tau_q \sim 5\mu s/P_{UF_6}$ at 500 °K where the UF_6 pressure is in atmospheres. Therefore, the larger the rate of rise of the neutron flux, the larger the density of excited HF is before this quenching time passes. Hence maximum gain will be proportional to the rate of rise of the neutron flux. Once τ_q has elapsed, the HF quenching rate is largest where the density of ground-state HF is the largest. Therefore, the length of time that gain is positive is inversely proportional to rate of pumping. This is illustrated in Fig. 2 where for a constant peak flux factor ($\Phi = 2 \times 10^{15}$ neutrons/cm^2 s) the FWHM of the neutron pulse was varied. Note that as the pulse width decreases, the peak gain increases and the time at which the gain is maximum decreases. The efficiency with which the neutron flux is used also increases with decreasing pulse width. The ratio of the flux factor at the time of maximum gain to the flux factor at its peak value has been termed the flux efficiency. The flux efficiency increases from less than 1% with a FWHM of $30\,\mu s$ to almost 10% with a FWHM of $200\,\mu s$.

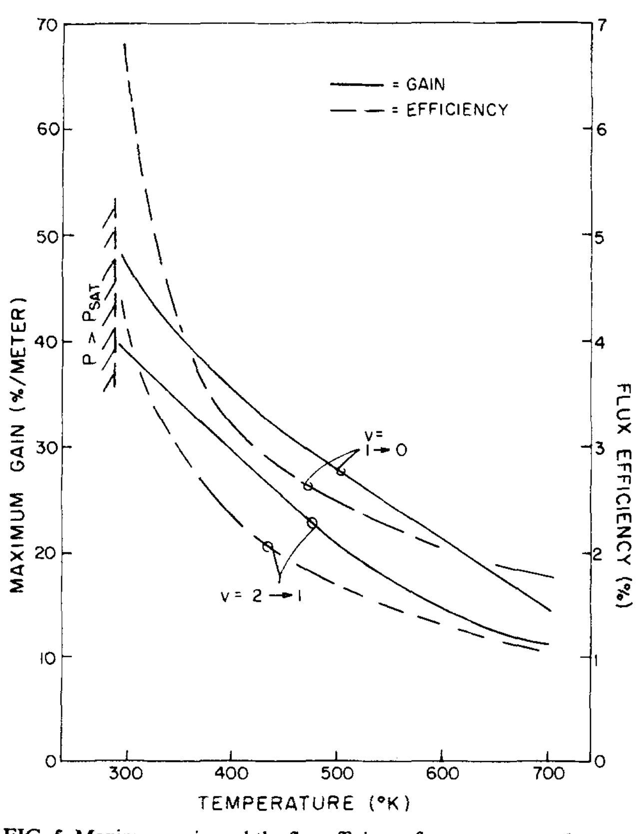

FIG. 5. Maximum gain and the flux efficiency for constant number densities as a function of initial gas temperature. The reference conditions are the same as for Fig. 1. Since the HF-HF VV quenching rate is endothermic, gain and flux efficiency increase as the gas temperatue decreases.

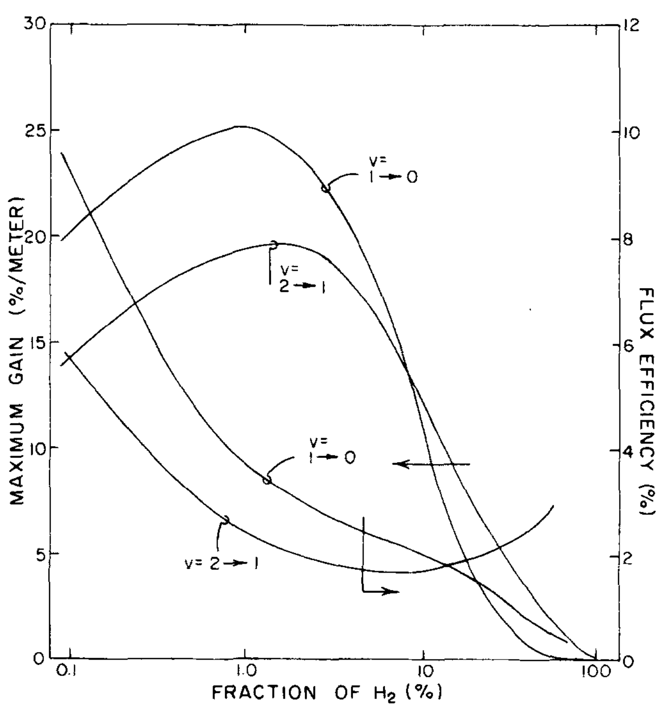

FIG. 6. Maximum gain as a function of the fraction of H_2. The total pressure is 0.4 atm. The peak flux factor is 2×10^{15} neutrons/cm^2 s and the neutron pulse width is $60\,\mu s$.

TABLE II. Threshold thermal neutron fluxes for present nuclear-pumped lasers.

Fission reaction	System	Lasant	Threshold thermal neutron flux ($/cm^2$ s)	Ref.
$^{10}B(n,\alpha)^7Li$	He-CO He-CO_2	C	4×10^{14}	3
$^{10}B(n,\alpha)^7Li$	Ne-N_2	N	1×10^{15}	2
$^3He(n,p)^3H$	He-Xe	Xe	4×10^{15}	9
$^{10}B(n,\alpha)^7Li$	He-Hg	Hg	10^{16}	1
$^3He(n,p)^3H$	He-Ar	Ar	1.4×10^{16}	8

When the neutron pulse width is held constant (60μs) and the peak flux factor is varied, similar results are obtained. Figure 3 shows maximum gain rising rapidly as the peak flux factor increases while the flux efficiency decreases. For a sufficiently small peak flux factor, the density of HF never becomes large so that the dominant quenching mechanism remains UF_6-HF VT collisions. Under these conditions, the gain is not abruptly quenched and the length of time which gain is positive approaches the length of the neutron pulse. (See Fig. 4.)

The threshold peak flux factor for an HF laser can be estimated from Fig. 3. The threshold pumping rate for a laser is that value at which gain for the photon flux equals losses. If the dominant loss mechanism is output coupling (cavity length $\approx$2m, output mirror reflectance $\approx$95%), then the threshold peak flux factor will be of the order of 5×10^{12} neutrons/cm^2 s. For $\alpha = 1.0$ and $\beta = 0.1$, the threshold peak flux is less than $10^{14}/cm^2$ s. The threshold flux can be further reduced by shortening the pulse width or decreasing the gas temperature (see below). This threshold flux is lower than any value reported to date. (See Table II.) The maximum gain calculated is comparable to any reported to date. (See Table III.)

We have seen that as long as UF_6-HF VT collisions are the dominant quenching mechanism, gain is proportional to the time-dependent flux factor. When VV collisions between ground-state and excited HF become the dominant mechanism, gain is quickly quenched. Since these collisions are endothermic, reducing the gas temperature will decrease their importance. Figure 5 illustrates the temperature dependence of maximum gain for constant initial number densities. The reference conditions are the same as for Fig. 1. Note the maximum gain increases roughly linearly as the initial gas temperature is reduced, and that the flux efficiency increases sharply. For temperatures below about 300 °K, the UF_6 pressure exceeds the saturated vapor pressure of UF_6 and therefore sets a lower limit (for a given UF_6 density) on the initial gas temperature.

TABLE III. Maximum gain reported for present nuclear-pumped lasers.

Fission reaction	System	Gain species	Maximum gain (%/m)	Ref.
$^3He(n,p)^3H$	He-Ne-O_2	O	0.9	7
$^{235}U(n,FF)FF$	CO-N_2-He-O_2	CO	35	27
$^3He(n,p)^3H$	He-Xe	Xe	200	28

For a given pressure, peak flux factor, and pulse width, there is an optimum fraction of H_2, which is around a few percent. Figure 6 shows the results of varying the fraction of H_2 for otherwise constant conditions. For values below optimum, the reaction which forms HF is limited by the small amount of H_2 present. As the fraction of H_2 is increased, more fission energy is deposited in the hydrogen instead of the UF_6. The rate of production of F decreases so that despite the abundance of H_2, the reaction rate for forming HF decreases (see Fig. 7). The length of time that gain is positive and the flux efficiency increases as the fraction of H_2 decreases.

The results discussed thus far have been for gain on the centerline of a tube whose radius is optimum. An optimum tube radius is one which exceeds the range of the fission fragments. Therefore, for a given pressure and gas composition there is a tube radius below which energy deposited on the centerline will decrease.[12] Alternately, one can consider the annular region adjacent to the wall of the tube with a thickness equal to the range of the fragments as a region where energy is not uniformly distributed. For points interior to this annular region, the energy deposition is uniform.

Figure 8 shows maximum gain for the $v = 1\rightarrow0$ transition as a function of pressure and tube radius. The peak flux factor is $2\times10^{15}/cm^2$ s and the neutron pulse width is $60\,\mu$s. The fraction of H_2 is 3%. Also shown in Fig. 8 is the maximum range of fission fragments for the gas mixture as a function of pressure. Note that the optimum pressure is around 0.35 atm, independent of the radius of the tube, but that the optimum gain decreases with decreasing radius as long as that radius is less than optimum. The precise value of the optimum pressure increase slightly with decreasing tube radius.

For pressures greater than about 0.3 atm, the vibrational-rotational transition is purely pressure broadened. There-

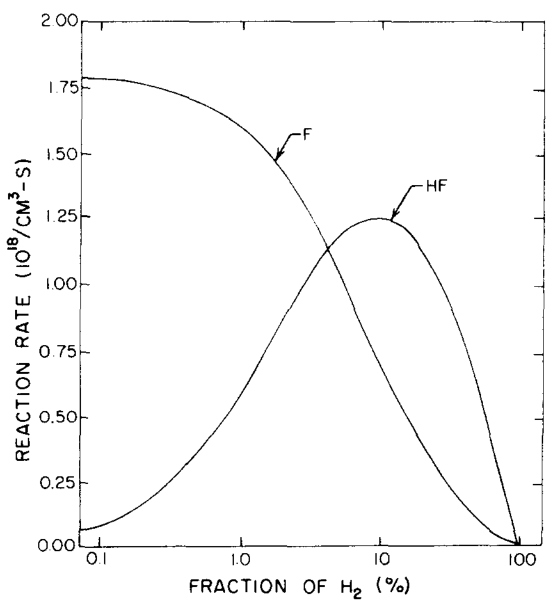

FIG. 7. Rate of production of HF due to reaction (2) and the rate of production of fluorine due to reaction (7) for the conditions of Fig. 6. The rate of production of HF is limited by the rate of production of fluorine as the hydrogen density increases.

fore, for otherwise constant conditions, a decrease in pressure results in an increase in the maximum value of the line-shape function $g(\nu)$ and hence gain is enhanced. Below about 0.3 atm, the transition to Doppler broadening begins, and the line-shape advantage gained by lowering the pressure is lost. Since the major quenching mechanism early during the neutron pulse is UF_6-VT collisions, lowering the pressure increases the quenching time τ_q, and delays the time when HF collisions become dominant. This is illustrated in Fig. 9 where the time at which gain for the $v = 1 \rightarrow 0$ transition is maximum is plotted as a function of pressure and tube radius. If the pressure is increased, the energy deposited in the gas and hence the pumping rate increase. But the increase in the pumping rate is insufficient to offset the decrease in τ_q and $g(\nu)$.

For pressures below about 0.35 atm the advantage gained with respect to decreasing quenching rates by lowering the pressure is smaller than the decrease in fission energy deposited and the decrease in the reaction rate that produces HF. This results in a decrease in maximum gain. For sufficiently low pressure, the range of fission fragments exceeds the radius of the tube. The rate at which energy is deposited and hence maximum gain decrease sharply.

The results discussed above are a function of the peak flux factor and temperature. Increasing the peak flux factor increases the optimum gain and shifts the optimum pressure to a lower value. Decreasing the gas temperature decreases the Doppler width and decreases the pressure at which the transition to Doppler broadening is made. This results in a lower optimum pressure and higher optimum gain.

IV. CONCLUDING REMARKS

A model for a nuclear-pumped UF_6-H_2/HF laser has been presented. The results show that this system potentially has the lowest neutron flux threshold of any nuclear pumped system to date ($< 10^{14}$ neutrons/cm^2 s), while the gain is comparable to any yet measured ($\gtrsim 50\%$/m). The gain is a sensitive function of the rate at which the neutron pulse rises. Because the gain is rapidly quenched, the rate of rise of the neutron pulse is more important than its peak flux. Therefore, threshold fluxes may be as much as an order of magnitude less than suggested here if the flux can be made to rise fast enough. The threshold rate of rise of the neutron flux is on the order of 10^{17}–10^{18} neutrons/cm^2 s^2. Optimum gain is obtained at the lowest temperature at which the optimum density is less than the saturation pressure of UF_6, and with a fraction of H_2 equal to a few percent.

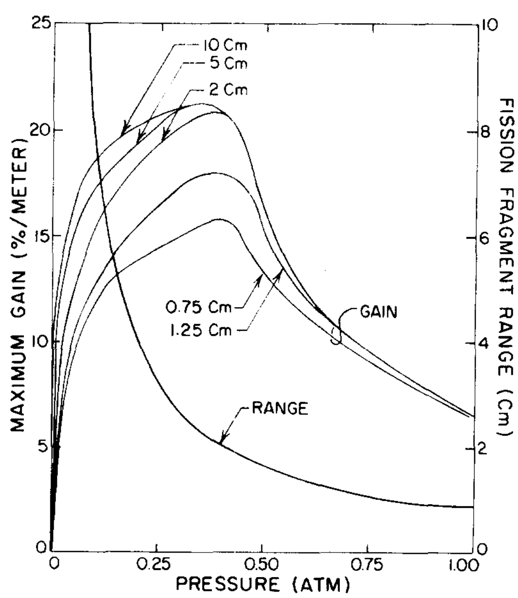

FIG. 8. Maximum gain for the $v = 1 \rightarrow 0$ transition as a function of total pressure and tube radius. The fraction of H_2 is 3%, and the peak flux factor is 2×10^{15} neutrons/cm^2 s. Also shown is the range of fission fragments as a function of pressure. At a given pressure, maximum gain decreases with decreasing tube radius as long as that radius is less than optimum.

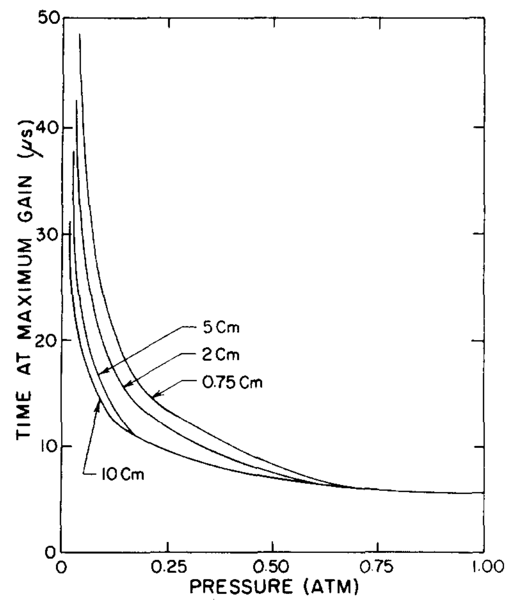

FIG. 9. Time after the start of the neutron pulse that gain is positive as a function of pressure and tube radius for the conditions of Fig. 8.

Present nuclear-pumped lasers, as well as the system proposed here, have relatively low gain. The motivation for their development should be because energy can be deposited uniformly in a large volume. This characteristic makes them attractive as amplifiers instead of oscillators. Consider an HF nulcear-pumped amplifier 1 meter in diameter and a few meters long. The output of an oscillator with a spot 1 cm in diameter is expanded, passed through the amplifier, and then contracted to its original size. The increase in intensity that the spot experiences would be equivalent to passing through an amplifier at its original radius which is many kilometers long.

Note added in proof: cw nuclear pumped lasing on the 6328-Å neon transition in a He-Ne system at 300 Torr has been recently reported [B.D. Carter, M.J. Rowe, and R.T. Schneider, Appl. Phys. Lett. **36**, 115 (1980)]. The threshold neutron flux was measured at 2×10^{11} neutrons/cm^2 sec.

ACKNOWLEDGMENTS

Computing funds were provided by the Caltech Division of Engineering and Applied Science. The author would like to acknowledge support by a Dr. Chaim Weizmann Postdoctoral Fellowship, and thank Dr. F.E.C. Culick and J.E. Shepherd for their comments.

[1] M.A. Akerman, G.H. Miley, and D.A. McArthur, Appl. Phys. Lett. **30**, 409 (1977).
[2] R.J. DeYoung, W.E. Wells, G.H. Miley, and J.T. Verdeyen, Appl. Phys. Lett. **28**, 519 (1976).
[3] M.A. Prelas, M.A. Akerman, F.P. Boady, and G.H. Miley, Appl. Phys. Lett. **31**, 428 (1977).
[4] D.A. McArthur and P.B. Tollefsud, Appl. Phys. Lett. **26**, 187 (1975).
[5] H.H. Helmick, J.L. Fuller, and R.T. Schneider, Appl. Phys. Lett. **26**, 327 (1975).
[6] J.C. Guyot, G.H. Miley, and J.T. Verdeyen, Nucl. Sci. Eng. **48**, 373 (1972).
[7] R.J. DeYoung, W.E. Wells, and G.H. Miley, Appl. Phys. Lett. **28**, 194 (1976).
[8] N.W. Jalufka, R.J. DeYoung, F. Hohl, and M.D. Williams, Appl. Phys. Lett. **29**, 188 (1976).
[9] R.J. DeYoung, N.W. Jalufka, and F. Hohl, Appl. Phys. Lett **30**, 19 (1977).
[10] J.W. Wilson, R.J. DeYoung, and W.L. Harries, J. Appl. Phys. **50**, 1226 (1979).
[11] N. Cohen, Aerospace Corporation Report No. TR-0073(3430)-9, 1973.
[12] J.W. Wilson and R.J. DeYoung, Appl. Phys. **49**, 980 (1978); **49**, 989 (1978).
[13] J.R. Lamarsh, *Introduction to Nuclear Reactor Theory* (Addison-Wesley, Reading, Mass. 1966).
[14] K.L. Kompa and G.C. Pimentel, J. Chem. Phys. **47**, 857 (1967).
[15] J.H. Parker and G.C. Pimentel, J. Chem. Phys. **51**, 91 (1979).
[16] K.L. Kompa, J.H. Parker, and G.C. Pimentel, J. Chem. Phys. **49**, 4257 (1968).
[17] J.K. Dawson, D.W. Ingram, and L.L. Bircumshaw, J. Chem. Soc. **30**, 1421 (1950).
[18] Reaction (17) is analogous to the reaction $H + SF_6 \rightarrow HF + SF_5$ with rate constant $r = 3\times10^{-9}e^{-}(30 \pm 5)\mathrm{kcal}/RT\ \mathrm{cm}^3/\mathrm{s}$. C.P. Fenimore and G.W. Jones, Combust. Flame **8**, 231 (1964).
[19] M.A. Kwok and N. Cohen, Aerospace Corporation Report No. TR-0075(5530)-8, 1975.
[20] J.M. Herbelin and G. Emanuel, Chem. Phys. **60**, 689 (1974).
[21] M.H. Rand and O. Kubashewski, *The Thermochemical Properties of Uranium Compounds* (Oliver and Boyd, Edinburgh, 1963).
[22] G.P. Verkhivker, S.D. Tetel'baum, and G.P. Konyaeva, Atom. Energiya **24**, 158 (1968).
[23] D.R. Stull and H. Prophet, *JANAF Thermochemical Tables*, 2nd ed. (NBS, Washington D.C., 1971).
[24] A. Yariv, *Quantum Electronics* (Wiley, New York, 1975).
[25] See, for example, H.A. Hassan and Jerry E. Deese, Phys. Fluids **19**, 2005 (1976).
[26] L.C. Northcliffe and R.F. Schillng, Nucl. Data Tables A **7**, 233 (1970).
[27] D.A. McArthur and P.B. Tollefsud, IEEE Quantum Electron **QE-12**, 244 (1976).
[28] R.J. DeYoung, N.W. Jalufka, and F. Hohl, AIAA J. **16**, 991 (1978).